Variation of nuclear magnetic shielding with intermolecular interactions and rovibrational motion. VII. ^{19}F in CF_2H_2, CF_2HCl, $CFHCl_2$, CF_2Cl_2, and $CFCl_3$

Cynthia J. Jameson
Department of Chemistry, University of Illinois at Chicago, Chicago, Illinois 60680

A. Keith Jameson
Department of Chemistry, Loyola University, Chicago, Illinios 60626

D. Oppusunggu
Department of Chemistry, University of Illinois at Chicago, Chicago, Illinois 60680

(Received 16 February 1984, accepted 21 March 1984)

Variable density and temperature studies of fluorine-19 nuclear magnetic resonance spectra in the title molecules reveal the effects of intermolecular interactions, quantitatively expressed as a second virial coefficient of nuclear shielding $\sigma_1(T)$ and the effects of rovibrational averaging, expressed in terms of the temperature dependence of shielding in the molecules in the zero-pressure limit $\sigma_0(T)$. The quantities are reported as quadratic functions of temperature and compared with those of other molecules. In the four series of molecules: (a) CH_3F, CF_2H_2, CF_3H, CF_4; (b) $CFCl_3$, CF_2Cl_2, CF_3Cl, CF_4; (c) CF_2Cl_2, CF_2HCl, CF_2H_2; and (d) $CFCl_3$, $CFHCl_2$, CFH_2Cl, CFH_3, $|d\sigma_0/dT|$ has been found to decrease with H substitution and increase with Cl substitution. Gas-to-liquid shifts are also reported.

INTRODUCTION

The nuclear magnetic shielding of a nucleus in a molecule in the dilute gas phase is an average value which is determined by rovibrational averaging in independent molecules as well as collisional averaging for pairs of interacting molecules. Provided the density is sufficiently low, binary interactions have dominant effects on shielding, resulting in an observed nuclear resonance frequency which is linearly related to density. At higher densities the nonlinear terms in the virial expansion of the nuclear magnetic shielding can become important. Thus, the nuclear shielding in the gas phase $\sigma(T,\rho)$ is as follows:

$$\sigma(T,\rho) = \sigma_0(T) + \sigma_1(T)\rho + \sigma_2(T)\rho^2 + \cdots .$$

In our previous studies of the ^{19}F nuclear shielding in the gas phase, we have reported $\sigma_0(T)$ and $\sigma_1(T)$ functions for ^{19}F in CF_4, CH_3F, CF_3H, and CF_3Cl, among others.[1-4] In this paper we report the density and temperature coefficients of the nuclear magnetic shielding in related molecules which form a series of compounds for which the effects of intermolecular interactions and rovibrational averaging can be compared. In so doing, we hope to have a better understanding of these effects. We report here the $\sigma_0(T)$ and $\sigma_1(T)$ for the *underlined* molecules in the following series:

CH_3F, $\underline{CH_2F_2}$, CF_3H, and CF_4, (a)

$\underline{CFCl_3}$, $\underline{CF_2Cl_2}$, CF_3Cl, and CF_4, (b)

$\underline{CF_2Cl_2}$, $\underline{CF_2HCl}$, $\underline{CF_2H_2}$, (c)

$\underline{CFCl_3}$, $\underline{CFHCl_2}$, CFH_2Cl, CFH_3. (d)

Together with our previous results on the other molecules, we now have complete $\sigma_0(T)$ information for all members of these four series of fluoromethanes (except for CFH_2Cl).

EXPERIMENT

^{19}F NMR spectra were taken at 84.7 MHz on a hybrid spectrometer consisting of a Bruker HFX-90 high resolution spectrometer and a Bruker B-KR 322 s pulsed spectrometer with a common 18 in. electromagnet at a nominal field strength of 21.15 kG and with rf-generating and pulse-gating frequencies derived from a common clock. With the inclusion of Nicolet 1080 data system, conventional pulsed Fourier transform spectra are acquired. Temperature regulation of the 5 mm sample assembly (sealed gas sample tube together with the lock substance toluene-d_8 in the annular region) was provided by a Bruker B-ST 100/700 variable temperature system. This system has been calibrated and is found to maintain a selected temperature to within $\pm$ 0.2°.

The sealed gas samples, ~0.2 ml volume, of 3.9 mm o.d., 2.2 mm i.d., 50 mm borosilicate tubing, are sufficiently small to minimize temperature gradients across the sample. Gases were obtained from Matheson and PCR Research Chemicals. The CD_3 group of toluene-d_8 provides the field-frequency lock. Toluene is an ideal lock substance in that it has the widest liquid range (178 to 383 K) and the chemical shift of the CD_3 signal with temperature is small and has been previously determined relative to atomic Xe.[5]

The ^{19}F nuclear resonance frequencies of four to eight samples (densities 1–40 amagat) of each gas were obtained from 380 K down to temperatures somewhat below the onset of liquefaction, and only the frequencies of the all-gas samples were used for the determination of σ_1. The resonance frequencies corresponding to data points below the condensation temperatures for each sample were plotted together and found to be coincident with the vapor curve obtained in the separate gas-to-liquid shift determination on a single sample. In the latter experiment, the sample was positioned in the receiver coil so as to observe both vapor and liquid in the same spectrum. In such an arrangement spinning side-

 0021-9606/84/130085-06$02.10

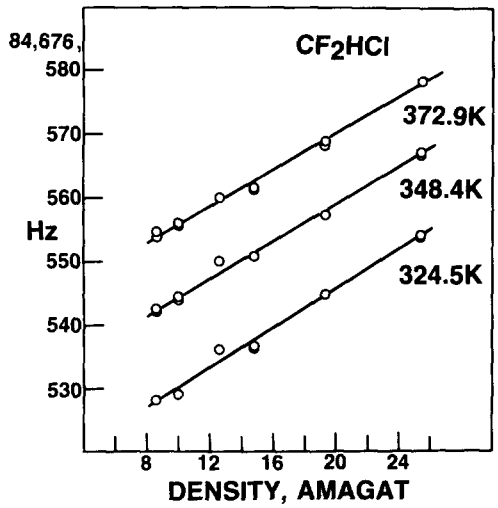

FIG. 1. The densitites of the gas samples are chosen to be sufficiently low so that at a given temperature the nuclear magnetic shielding is linearly dependent on density, shown typically by ^{19}F in CF_2HCl. The slopes of these lines give the value of σ_1 at that temperature.

bands for the liquid complicate the spectrum. However, by varying the spinning rate, the liquid (and vapor) resonance frequencies could be determined without ambiguity. The liquid signal was observed through lower temperatures, and the equilibrium vapor signal through higher temperatures beyond the range in which both signals appear in the spectra. The temperature for onset of liquefaction for each sample was found to be consistent with the known equilibrium vapor density curves of the title molecules.[6–8]

RESULTS

Effects of intermolecular interactions

The effects of intermolecular interactions on nuclear magnetic shielding are contained in the density dependent part of the nuclear resonance frequencies. In this work, we have studied these effects in two ways. First, we have measured the resonance frequencies in the dilute gas phase in samples of various known densities. The densities are chosen to be low enough so that only binary interactions contribute to the shielding, giving a linear plot of resonance frequencies vs densities at a given temperature. From these, we found $\lim_{\rho\to 0}(\partial\nu/\partial\rho)_T$. Second, we have measured the shielding difference between the neat liquid and the vapor in equilibrium with it. In taking the difference at any given temperature, the rovibrational averaging effects subtract out, provided that the molecule undergoes the same rovibrational averaging in the liquid phase as in the dilute gas phase, leaving only the density dependent effects from binary and higher order interactions. The advantage of the second type of measurement is that one obtains frequency differences due to density differences which are an order of magnitude larger than in the all-gas-phase systems. The extent to which these data (which include the effect of many-body interactions) can be compared to data in the binary-interactions regime remains to be seen.

Both the $\sigma_1 = \lim_{\rho\to 0}(\partial\sigma/\partial\rho)_T$ and the $(\sigma_{\mathrm{LIQ}} - \sigma_{\mathrm{VAP}})(T)$, which we have measured for the ^{19}F nuclei in the title molecules, include uninteresting contributions due to bulk susceptibility. That part of the nuclear shielding experienced by a nucleus in a molecule in a gas or liquid in a cylindrical sample tube with the axis of the cylinder perpendicular to the

TABLE I. The observed second virial coefficient of ^{19}F nuclear magnetic shielding in various gases, $\sigma_1(T)$ and $(\sigma_1 - \sigma_{1b})$ for interaction between like pairs of molecules, in ppb/amagat.

Molecule	T(K)	$\sigma_1(T)$	χ (10^{-6}cm^3/mol)	σ_{1b}	$(\sigma_1 - \sigma_{1b})$ at 300 K
CF_2Cl_2	330–380	$-(21.71 \pm 1.69) + 6.69\times10^{-3}(T\text{-}300)$	-52.2[f]	-4.88	-16.8
$CFCl_3$	350–380	$-(21.26 \pm 1.74)$	-58.67[f]	-5.48	-15.8 (at 350)
CF_2HCl	300–380	$-(17.16 \pm 0.89)$	-38.6[f]	-3.61	-13.6
$CFHCl_2$	350–380	$-(25.17 \pm 1.35)$	-48.8[f]	-4.56	-21.6
CF_2H_2	300–380	$-(7.06 \pm 1.06)$	-24.5[h]	-2.29	-4.8
CFH_3	280–380	$-(15.70 \pm 1.8) + 2.62\times10^{-2}(T\text{-}300)$[a]	-21.1[d]	-1.97	-13.7
CF_3H	240–380	$-(9.40 \pm 0.67) + 4.00\times10^{-2}(T\text{-}300)$[b]	-28.3[e]	-2.64	-6.8
CF_4	270–410	$-(11.55 \pm 0.31)$[c]	-31.0[f]	-2.90	-8.65
CF_3Cl	220–380	$-(19.93 \pm 1.8) + 3.65\times10^{-2}(T\text{-}300)$[g]	-45.3[f]	-4.23	-15.70

[a] Reference 2. This is a corrected value.
[b] Reference 4.
[c] Reference 1.
[d] Calculated from Pascal constants, in good agreement with -20.8×10^{-6} cm^3/mol calculated with Haberditzl's method by Beran and Kevan (Ref. 13).
[e] L. Petrakis and H. J. Bernstein, J. Chem. Phys. 37, 2731 (1962).
[f] Experimental values: G. Foex, *Tables de Constantes et Donnees Numerique I Constantes Selectionees Diamagnetisme et Paramagnetisme* (Masson et Cie, Paris, 1957).
[g] C. J. Jameson and A. K. Jameson, J. Chem. Phys. (to be published).
[h] Calculated from Pascal constants, in good agreement with -24.8×10^{-6} cm^3/mol calculated with Haberditzl's method by Beran and Kevan (Ref. 13).

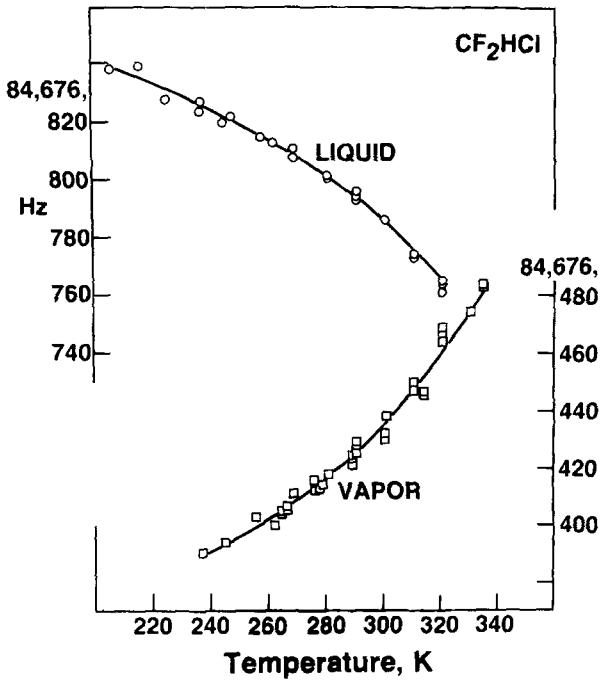

FIG. 2. The resonance frequencies of both the liquid phase and the vapor in equilibrium with it can be measured from the same spectrum. A typical result is shown here for CF_2HCl. The functional forms of liquid and vapor curves such as these are given in Table II.

magnetic field is given by $(2\pi\chi/3)\rho$, where χ is the molecular magnetic susceptibility.

The typical all-gas data from which we obtain σ_1 are shown in Fig. 1. The resonance frequencies vs density plots are linear and their slopes give a measure of σ_1. The molecular magnetic susceptibilities for these molecules have been used to obtain the bulk susceptibility contribution to σ_1, and by difference, the pair-interaction contribution to σ_1, i.e., $(\sigma_1-\sigma_{1b})$. These are compared with values for related molecules in Table I. The measured value of σ_1 was nearly constant over the entire temperature range for several gases. A definite temperature dependence was observed for σ_1 only in CF_2Cl_2, $|\sigma_1|$ decreases with increasing temperature. This is the usually observed trend for all other ^{19}F nuclei for which $\sigma_1(T)$ has been measured.[9]

The simultaneous observation of the ^{19}F resonance in the liquid and the vapor in equilibrium with it results in curves such as those shown in Fig. 2 for CF_2HCl. For all the systems studied here, the resonance frequency of a nucleus in the liquid phase has basically the same behavior with temperature: It is characterized by negative first and second derivatives of frequency with temperature. The resonance frequency decreases with increasing temperature due primarily to the decrease in density upon expansion of the liquid. This is consistent with the decrease of the resonance frequency with decreasing sample density observed in the all-gas samples (as in Fig. 1). On the other hand, the equilibrium vapor curves are characterized by positive first and second derivatives of frequency with temperature. The resonance frequency increases with increasing temperature, primarily due to the increase in vapor density with the exponential increase in

TABLE II. Temperature dependence of ^{19}F nuclear resonance in the liquid phase and in the vapor in equilibrium with it. The experimental data can be adequately described by the following functions valid only in the temperature ranges indicated: $\nu_{LIQ}(T)=\nu_{LIQ}(T_0)+a_1(T-T_0)+a_2(T-T_0)^2$ (Hz); $\nu_{VAP}(T)=\nu_{VAP}(T_0)+b_1(T-T_0)+b_2(T-T_0)^2$ (Hz); $(\sigma_{LIQ}-\sigma_{VAP})(T)=c_0+c_1(T-T_0)+c_2(T-T_0)^2$ (ppm). The gas-to-liquid shifts due to bulk susceptibilities are shown in the same functional form, for the same range of temperatures.

Molecule	T_0 (K)	T(K)	$\nu_{LIQ}(T)^a$ a_1	10^3a_2	T(K)	$\nu_{VAP}(T)^a$ b_1	10^3b_2	T(K)	$(\sigma_{LIQ}-\sigma_{VAP})(T)$ c_0	10^2c_1	10^4c_2	Bulk susc. contrib (ppm[b]) d_0	10^2d_1	10^4d_2
CF_2Cl_2	300	236–327	−0.904	−2.33	270–330	+1.311	+4.78	277–327	−5.154	+2.62	+0.84	−1.146	+0.43	+0.29
$CFCl_3$	340	258–370	−0.350	−1.43	311–380	+1.27	+2.92	310–370	−5.994	+1.91	+0.51	−1.207	+0.29	+0.08
CF_2HCl	300	207–321	−0.940	−3.44	237–335	+1.119	+7.10	237–321	−4.140	+2.43	+1.24	−1.064	+0.48	+0.16
$CFHCl_2$	300	227–342	−0.307	−1.31	280–380	+0.848	...	280–345	−5.972	+1.36	+0.15	−1.345	+0.27	+0.08
CF_2H_2	280	220–300	−0.758	−2.67	232–300	+0.480	+4.30	230–300	−3.172	+1.53	+1.08	−1.023	+0.40	+0.13

[a] These have not been corrected for the slight temperature dependence of the lock substance, toluene-d_8, which is known (Ref. 5).
[b] Calculated by $(2\pi/3)\chi(\rho_{LIQ}-\rho_{VAP})(T)$ using χ values given in Table I, liquid and vapor densities from Landolt-Bornstein (Ref. 6) for CF_2HCl, $CFHCl_2$, CF_2Cl_2, $CFCl_3$, Ref. 7 for $CFHCl_2$, $CFCl_3$, and Ref. 8 for CF_2H_2.

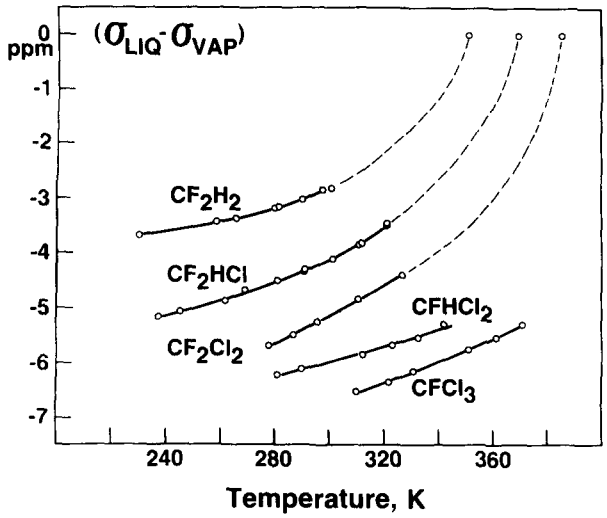

FIG. 3. The measured gas-to-liquid shifts $(\sigma_{LIQ} - \sigma_{VAP})(T)$ shown above are represented as quadratic functions of temperature in Table II. They are partly (~ 20%) due to the bulk susceptibility difference, also given in Table II. The gas-to-liquid shift goes to zero at the critical temperature, indicated in the figure for CF_2H_2 (351 K), CF_2HCl (369 K), and CF_2Cl_2 (385 K). $CFHCl_2$ and $CFCl_3$ have much higher critical temperatures: 451.5 and 471 K, respectively. All critical data are from the references cited in Table II.

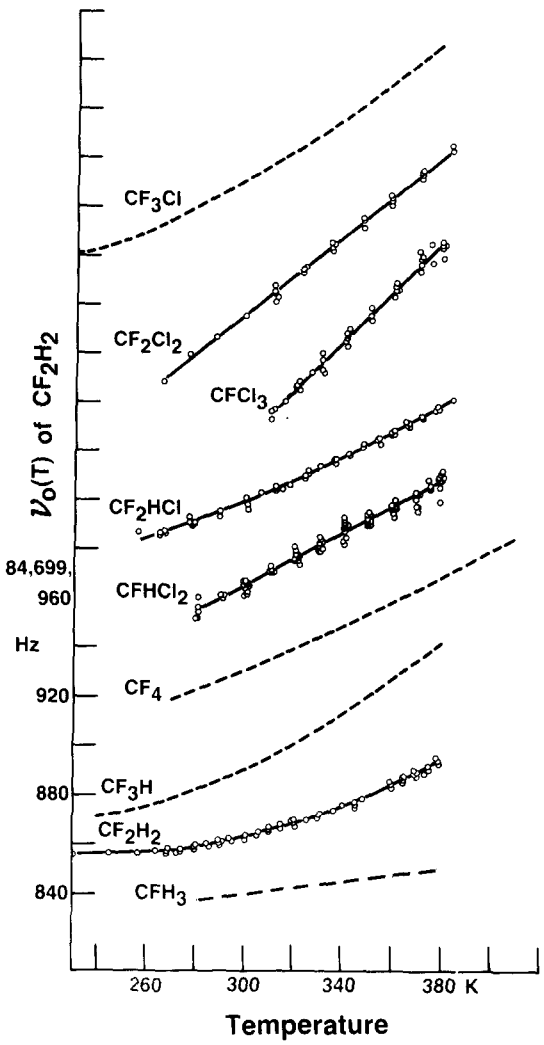

FIG. 4. The resonance frequencies of each sample corrected for intermolecular effects ($\sigma_1\rho$ is subtracted out) and for the slight temperature dependence of the lock substance, toluene-d_8, represent the resonance frequency, $\nu_0(T)$ of the isolated molecule. The above results are represented by the functions $[\sigma_0(T) - \sigma_0(300)]$ which are given in Table I. Dashed lines trace the functional form for related molecules, which have been previously reported for CF_4 (Ref. 1) and for CF_3H and CF_3Cl (Ref. 3). For CFH_3, Ref. 2, this should be $[\sigma_0(T) - \sigma_0(300)]_{CFH_3} = -1.515(T\text{-}300)$ ppb for $T = 280$–380 K.

vapor pressure as the temperature increases. Again, this is consistent with Fig. 1. These experimental curves can be described by quadratic functions of temperature, as in Table II.

In addition to the effects of the variation in density, both liquid and vapor curves contain the intrinsic change of the resonance frequency and rovibrational averaging for the isolated molecule, which subtracts out when the shielding difference is taken. The gas-to-liquid shift is conveniently expressed as the shielding difference $(\sigma_{LIQ} - \sigma_{VAP})(T)$. These are plotted in Fig. 3 and described by quadratic functions of temperature in Table II. Each of the $(\sigma_{LIQ} - \sigma_{VAP})$ curves shown in Fig. 3 should approach zero at the critical temperature. We can see that this is consistent with the curves for CF_2H_2, CF_2HCl, and CF_2Cl_2, for which $(\sigma_{LIQ} - \sigma_{VAP})(T)$ could easily go to zero at 351, 369, and 385 K, respectively.[6,8] $CFHCl_2$ and $CFCl_3$ have much higher critical temperatures, 451.5 and 471 K, respectively.[6] Their curves are not inconsistent with the gas-to-liquid shift becoming zero at these temperatures. The shielding differences $(\sigma_{LIQ} - \sigma_{VAP})(T)$ are primarily (~80%) due to intermolecular interactions. The uninteresting part (~20%) due to the bulk susceptibility contribution to the gas-to-liquid shift is calculated from the liquid and vapor densities as $(2\pi\chi/3)(\rho_{LIQ} - \rho_{VAP})(T)$, where the molecular magnetic susceptibility χ is assumed to be temperature independent. It should be noted that this bulk susceptibility contribution to the shift (given in Table II) is valid only for the sample geometry used here, in which the cylindrical sample has its axis perpendicular to the magnetic field. In NMR spectrometers with superconducting magnets, the cylindrical samples will have a bulk susceptibility contribution to the gas-to-liquid shift which is a factor (− 2) times the values shown in Table II.

Effects of rovibrational averaging

That the plots in Fig. 1 are linear indicates that when $\sigma_1(T)\rho$ is subtracted from the observed frequencies, the data points from all samples at the same temperature should become coincident. After the resonance frequencies measured as a function of temperature for each sample are corrected for intermolecular effects in this way, the resulting frequencies of the samples drop to a common curve, the resonance frequencies characteristic of the independent molecule $\nu_0(T)$. This is a zero pressure or an "isolated molecule" limit in the sense that sufficient collisions occur to allow the molecule to average the nuclear shielding σ over the molecular rotational and vibrational states but not enough to cause an intermolecular chemical shift. These zero-pressure-limit curves are shown in Fig. 4. The vapor resonance frequencies from the gas-to-liquid shift experiment and the vapor data for the var-

ious gas samples after onset of liquefaction also contain the same $\sigma_0(T)$ information as the all-gas data. When $\sigma_1(T)\rho_{VAP}(T)$ correction is made on each vapor resonance frequency, the $\nu_0(T)$ frequencies so obtained coincide with those obtained from the all-gas samples. Thus, Fig. 4 includes these vapor points as well. From these $\nu_0(T)$ curves, the functions $[\sigma_0(T) - \sigma_0(300)]$ have been obtained, and are given in Table III.

For some molecules, $[\sigma_0(T) - \sigma_0(300)]$ is fitted to a quadratic function of temperature, since some curvature was apparent in the range of temperatures studied. For others the precision of the data and range of temperatures studied warrant only a linear fit. In all cases the polynomial functions are valid only in the limited range of temperature indicated in Table III. These curves have the usual behavior with temperature: in the isolated molecule the resonance frequency increases (the nuclear shielding decreases) with increasing temperature, $d\sigma_0/dT$ is negative. This is typical of all the systems studied so far, except for ^{15}N and ^{31}P in NH_3 and PH_3, respectively.[9]

In Fig. 4, the curves previously reported for related molecules have been drawn as dashed lines so that the comparisons can be made visually for the four series of fluoromethanes which we consider here. The values of $(d\sigma_0/dT)_{T=300}$ for the ^{19}F in the series CFH_3, CF_2H_2, CF_3H, CF_4 are -1.515,[2] -2.76, -5.60,[4] -5.01[1] ppb deg^{-1}, respectively. For the series $CFCl_3$, CF_2Cl_2, CF_3Cl, CF_4, these values are -12.0, -9.36, -6.78,[4] -5.01[1] ppb deg^{-1}. For the third series CF_2Cl_2, CF_2HCl, CF_2H_2, these values are -9.36, -4.86, -2.76. For the last series $CFCl_3$, $CFHCl_2$, CFH_2Cl, CFH_3 they are -12.0, -6.22, (not measured), -1.515[2] ppb deg^{-1}. For all four series of fluoromethanes we note a decrease of $|d\sigma_0/dT|$ with substitution and an increase of $|d\sigma_0/dT|$ with Cl substitution.

The coupling constants observed, ^2J(HF) in CF_2HCl and in $CFHCl_2$ agree with literature values.[10] They are 50.5 Hz for CH_2F_2, 63.7 Hz for CF_2HCl, and 54. Hz for $CFHCl_2$. Any variation of ^2J (HF) with temperature or density was within our experimental errors, and no attempt was made to determine the coupling constant to better than 0.3 Hz.

DISCUSSION AND CONCLUSIONS

The effects on nuclear shielding due to binary intermolecular interactions $(\sigma_1 - \sigma_{1b})$, which we report here for the series of fluoromethanes, cover a fourfold range: -4.8 to -21.6 ppb/amagat. The combination of binary and many-body collision effects, measured in the form of gas-to-liquid shifts, $(\sigma_{LIQ} - \sigma_{VAP})$ can be converted to the same dimensions as σ_1 by dividing by $(\rho_{LIQ} - \rho_{VAP})$. When corrected for the bulk susceptibility contribution, the values of $(\sigma_{LIQ} - \sigma_{VAP})(T)/(\rho_{LIQ} - \rho_{VAP})$ at 300 K are surprisingly similar to those of $(\sigma_1 - \sigma_{1b})$ obtained from the dilute gas phase. These values are -16.8 and -17.4 for CF_2Cl_2, -15.8 and -21.5 for $CFCl_3$ (at 350 K), -13.6 and -10.2 for CF_2HCl, -21.6 and -15.7 for $CFHCl_2$, and -4.8 and -5.0 ppb/amagat for CF_2H_2 for $(\sigma_1 - \sigma_{1b})$ and $(\sigma_{LIQ} - \sigma_{VAP})/(\rho_{LIQ} - \rho_{VAP})$, respectively. The pairs of values agree within experimental error in cases of CF_2Cl_2 and CF_2H_2, and the other pairs are reasonably close. The differences between these pairs of values are due to many-body effects, and appear to be small compared to the magnitude of the two-body effect $(\sigma_1 - \sigma_{1b})$. Furthermore, the many-body effects appear to be opposite in sign to the two-body effects in most cases. This finding is consistent with the observation in xenon gas that at low densities, the ^{129} Xe resonance frequency increases linearly with density but tends to increase less at higher densities,[11] that is, in xenon gas, the sum of the $\sigma_2(T)\rho^2 + \cdots$ terms are opposite in sign to $\sigma_1(T)\rho$. We may consider $(\sigma_{LIQ} - \sigma_{VAP})/(\rho_{LIQ} - \rho_{VAP})$ as an "effective σ_1" for the liquid phase. If this quantity were independent of temperature, the $(\sigma_{LIQ} - \sigma_{VAP})(T)$ curves would be the density difference curves $(\rho_{LIQ} - \rho_{VAP})(T)$ scaled by a constant factor.

We postpone detailed consideration of the $(\sigma_1 - \sigma_{1b})$ values reported here in terms of the theory of intermolecular effects on nuclear shielding, such as the theory of Raynes, Buckingham, and Bernstein;[12] however, we can examine the contributing factors briefly. Raynes,Buckingham, and Bernstein (RBB) considered the following contributions to σ_1:

$$\sigma_1 = \sigma_{1b} + \sigma_{1w} + \sigma_{1E} + \sigma_{1a}.$$

We have already taken into account the uninteresting bulk susceptibility term σ_{1b}. The van der Waals term σ_{1w} includes effects of both repulsion and dispersion, although only the dispersion effects have been modeled as $\sigma_{1w} = -B\langle R^{-6}\rangle^T \alpha_2 I_2/(I_1 + I_2)$, in which B is a property of the nucleus in question, α_2 is the electric dipole polarizability of the collision partner, I_1 and I_2 are the ionization energies of the molecule and its collision partner. σ_{1E} is the electrical contribution to the intermolecular effects on nuclear shielding, such as the effects of electric dipole–dipole, dipole-induced dipole, dipole–quadrupole, etc. interactions. σ_{1a} is the contribution to nuclear shielding due to the magnetic anisotropy of the collision partner. It is interesting to note that the magnitudes of $(\sigma_1\text{-}\sigma_{1b})$ are larger for molecules with larger electric dipole polarizabilities. $(\sigma_1 - \sigma_{1b}) = -15.8$ to -21.6 ppb/amagat for those with polarizabilities[13] 45.8 to 82.8×10^{-25} cm^3 ($CFCl_3$, CF_2Cl_2, CF_3Cl, CF_2HCl, $CFHCl_2$); $(\sigma_1 - \sigma_{1b}) = -4.8$ to -8.65 ppb/amagat for those with polarizabilities 26.5 to 27.3×10 cm^3 (CF_2H_2, CF_3H, CF_4). This correlation is to be expected from the van der Waals term in the RBB model. The exception is CFH_3 which has a larger $(\sigma_1 - \sigma_{1b})$ than expected with a lower polarizability $(26.0\times10^{-25}$ cm^3). However, this molecule also has a fairly large molecular electric dipole moment. Thus electric dipole–dipole contributions to σ_{1E} may

TABLE III. Temperature dependence of the ^{19}F nuclear magnetic shielding in the zero-pressure limit.

Molecule	T(K)	$[\sigma_0(T) - \sigma_0(300)]$(ppb)
CF_2Cl_2	265–380	$-9.06(T\text{-}300)$
$CFCl_3$	310–380	$-11.65(T\text{-}300)$
CF_2HCl	255–380	$-4.86(T\text{-}300) - 1.19\times10^{-2}(T\text{-}300)^2$
$CFHCl_2$	280–380	$-5.92(T\text{-}300)$
CF_2H_2	230–380	$-2.89(T\text{-}300) - 1.69\times10^{-2}(T\text{-}300)^2$

be important in addition to the van der Waals terms σ_{1W} to account for the $(\sigma_1 - \sigma_{1b})$ value of -13.7 ppb/amagat.

The effects of rovibrational averaging on nuclear magnetic shielding or any other molecular electronic property can be interpreted in terms of the change in the property with molecular configuration. An expansion of σ in terms of nuclear displacements from the equilibrium positions can be expressed in powers of the normal coordinates q_i:

$$\sigma_0(T) = \sigma_e + \sum_i (\partial\sigma/\partial q_i) < q_i >^T + \cdots.$$

The observed change in σ_0 is then attributed to sums over terms with an electronic structural factor $(\partial\sigma/\partial q_i)_e$, and a dynamic average of a coordinate $\langle q_i \rangle^T$. The relationship between normal vibrational coordinates q_i and bond extensions Δr_{CF}, or angle deformation $\Delta\alpha_{FCX}$ (derived from a normal coordinate analysis for the molecules) also allows us to write $\sigma_0(T)$ in terms of products $(\partial\sigma^F/\partial\Delta r_{CF})\langle\Delta r_{CF}\rangle^T + \cdots$ The temperature dependence of $\sigma_0(T)$ is contained in the thermal averages $\langle\Delta r_{CF}\rangle^T$, $\langle(\Delta r_{CF})^2\rangle^T$, $\langle(\Delta\alpha_{FCX})^2\rangle^T$, etc., with the intensity factors such as $(\partial\sigma/\Delta\alpha_{CF})_e$, which give the change in nuclear shielding arising from the change in electronic distribution upon bond displacement. We have already shown that the anharmonic contributions to $\langle\Delta r\rangle^T$ are largely responsible for the $(d\sigma_0/dT)$ observed in diatomic molecules.[14] Furthermore, Ditchfield has confirmed this with his calculations on selected diatomic molecules.[15] For molecules such as the methane derivatives studied here, the contributions by bond angle deformations such as the term $(\partial\sigma/\partial\Delta\alpha)_e\langle\Delta\alpha_{FCX}\rangle^T$ are probably not as important as the contributions by CF bond extensions: $(\partial\sigma_F/\partial\Delta r_{CF})_e\langle\Delta r_{CF}\rangle^T$. The near tetrahedral equilibrium geometry implies that the effect of angle deformations will largely cancel each other, so that their contribution to the thermal average $\sigma_0(T) - \sigma_e$ will be small compared to the contribution of $\langle\Delta r_{CF}\rangle^T$ terms.

Our results show a decrease of $d\sigma_0/dT$ with H substitution and an increase with Cl substitution for all four series of fluoromethanes. The nature of the dynamic (anharmonic) averaging varies a great deal from series to series as the relative masses of substituents and molecular symmetries change. That the trends in $d\sigma_0/dT$ upon H or Cl substitution are consistent in all four series, notwithstanding differences in molecular symmetry, must mean that the influence of Cl (or H) substitution on $(\partial\sigma^F/\partial\Delta r_{CF})$ magnitudes is more important than the effect on the dynamic average of $\langle\Delta r_{CF}\rangle^T$. This implies a systematic effect of such substitution on $(\partial\sigma^F/\langle\Delta r_{CF}\rangle)_e$. It is therefore of interest to calculate, even semiempirically, the ^{19}F nuclear shielding in a few molecules of these series, to see if this is indeed the case. The systematic trends in $d\sigma_0/dT$ with H or Cl substitution do not rule out additional systematic effects of mass changes on the vibrational averaging. To estimate these dynamic effects, it would be helpful to be able to compare even the root mean square vibrational amplitudes $\langle(\Delta r_{CF})^2\rangle^{1/2}$ obtained from electron diffraction data on these molecules. Unfortunately there are only isolated data of this nature (for CF_4, CF_3Cl, CF_2H_2 of these series of molecules) which have been compiled.[16]

In summary, we have reported the effects of intermolecular interaction of F nuclear shielding as measured in the dilute gas phase in the form of the second virial coefficient of nuclear shielding σ_1, as well as the gas-to-liquid shift. Our results are consistent with known information about these systems (vapor densities, critical data, molecular data such as polarizabilities), with known intermolecular effects on nuclear shielding in other F systems, as well as with such effects previously observed in other nuclei. Furthermore, the results are qualitatively consistent with existing (RRB) theory of these effects. More detailed calculations will be necessary in order to interpret $(\sigma_1 - \sigma_{1b})$ quantitatively.

We have also reported the temperature dependence of rovibrationally averaged ^{19}F nuclear shielding in the isolated molecules CF_2H_2, CF_2HCl, $CFHCl_2$, CF_2Cl_2, and $CFCl_3$. By comparing related molecules in four series of fluoromethanes, we note systematic effects of H and Cl substitution on the temperature coefficient of nuclear shielding. The latter is dependent on two factors: the electronic factor $(\partial\sigma_F/\partial\Delta r_{CF})$ and the dynamic factor, the thermal average of $\langle\Delta r_{CF}\rangle$. We believe that H and Cl substitution systematically affects $(\partial\sigma^F/\partial\Delta r_{CF})$ via the usual shielding dependence on electronic structure of a molecule. We suggest that theoretical calculation of σ for F nuclei in a series of these fluoromethanes is in order, as is a calculation of the dynamic average $\langle\Delta r_{CF}\rangle$ from the intramolecular force fields of these molecules.

ACKNOWLEDGMENT

This research was supported in part by The National Science Foundation (Grant CHE81-16193).

[1] C. J. Jameson, A. K. Jameson, and S. M. Cohen, J. Chem. Phys. **67**, 2271 (1977).
[2] C. J. Jameson and A. K. Jameson, J. Chem. Phys. **69**, 1655 (1978).
[3] C. J. Jameson, A. K. Jameson, and H. Parker, J. Chem. Phys. **69**, 1318 (1978).
[4] C. J. Jameson, A. K. Jameson, and H. Parker, J. Chem. Phys. **70**, 5916 (1979).
[5] C. J. Jameson, A. K. Jameson, and S. M. Cohen, J. Chem. Phys. **65**, 3397 (1976).
[6] *Landolt–Bornstein Tables*, 6th ed. (Springer, Berlin, 1967), Vol. 4, Part 4a.
[7] N. B. Vargaftik, *Tables on the Thermophysical Properties of Liquids and Gases*, 2nd ed. (Wiley, New York, 1975).
[8] P. F. Malbrunot, P. A. Meunier, G. M. Scatena, W. H. Mears, K. P. Murphy, and J. V. Sinka, J. Chem. Eng. Data **13**, 16 (1968).
[9] C. J. Jameson, Bull. Magn. Reson. **3**, 3 (1980).
[10] J. W. Emsley, L. Phillips, and V. Wray, Prog. NMR Spectrosc. **10**, 83 (1975); V. Wray, Ann. Rep. NMR Spectrosc. B **10**, 1 (1980).
[11] C. J. Jameson, A. K. Jameson, and S. M. Cohen, J. Chem. Phys. **59**, 4540 (1973).
[12] W. T. Raynes, A. D. Buckingham, and H. J. Bernstein, J. Chem. Phys. **36**, 3481 (1962).
[13] J. A. Beran and L. Kevan, J. Phys. Chem. **73**, 3860 (1969).
[14] C. J. Jameson, J. Chem. Phys. **66**, 4977 (1977).
[15] R. Ditchfield, Chem. Phys. **63**, 185 (1981).
[16] S. J. Cyvin, *Molecular Vibrations and Mean Square Amplitudes* (Elsevier, Amsterdam, 1968).